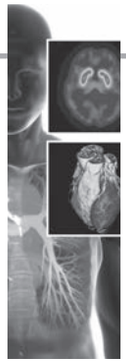

# Real-time MRI: recent advances using radial FLASH

Recent advances in real-time MRI result in high-quality images with acquisition times of only approximately 30 ms. The technique employs a fast low-angle shot sequence with proton density, $T_1$ or $T_2/T_1$ contrast and radial data encoding for motion robustness. High temporal resolution is achieved by an up to 20-fold undersampling of the radial data. An iterative reconstruction algorithm estimates the image as the solution of a nonlinear inverse problem and ensures image fidelity by temporal regularization, which exploits the temporal continuity of successive frames during dynamic imaging. Preliminary real-time examinations at a field strength of 3T range from joint dynamics, speaking and swallowing to the 3D localization of objects in space. In particular, real-time MRI largely facilitates assessments of cardiovascular function and quantitative blood flow. Taken together, advanced real-time MRI methods allow for hitherto inaccessible studies, lead to more robust and shorter examinations, improve patient comfort and offer new diagnostic opportunities.

**KEYWORDS: cardiovascular MR ■ dynamic imaging ■ MRI ■ nonlinear inverse reconstruction ■ real-time imaging ■ speaking ■ swallowing**

**Martin Uecker[1], Shuo Zhang[1], Dirk Voit[1], Klaus-Dietmar Merboldt[1] & Jens Frahm*[1]**

*[1]Biomedizinische NMR Forschungs GmbH am Max-Planck-Institut für biophysikalische Chemie, 37070 Göttingen, Germany*
**Author for correspondence: Tel.: +49 551 201 1721 jfrahm@gwdg.de*

MRI in real time is neither a recent desire nor a modern concept, but almost as old as the history of MRI. As early as 1984–1985, well before the advent of major industrial developments, widespread access to superconducting whole-body magnets, and promising clinical trials in neuroimaging, Sir Peter Mansfield and colleagues in Nottingham (UK) used echo-planar imaging to perform real-time or at least snapshot MRI studies of the thorax in animals and young children [1,2].

The subsequent invention of fast low-angle shot (FLASH) gradient echo MRI in 1985 [3] with its at least 100-fold gain in acquisition speed compared with established MRI sequences vastly broadened the spectrum of clinical MRI examinations and even allowed for preliminary studies of dynamic processes such as turbulent flow – although at still very limited temporal resolution [4]. Also, dynamic imaging of the heart became possible for the first time, but required a synchronization of the acquisition process with the ECG – often in conjunction with breath holding. Further improvements in cardiovascular MRI as the most demanding application with respect to speed rely on retrospective gating techniques that exploit simultaneous recordings of respiratory or ECG signals. However, the quality of most approaches still suffers for patients who present with cardiac arrhythmia or are unable to hold their breath. This problem is often emphasized by the fact that most MRI sequences employ a phase-encoding magnetic field gradient along at least one spatial dimension.

In the past two decades, major progress in MRI methodology involved technical improvements of the radiofrequency (RF) and magnetic field gradient systems, the implementation of parallel imaging [5,6], experimentation with non-Cartesian encoding strategies such as spiral [7,8] or radial trajectories [9–12], and the adaptation of advanced mathematical concepts for image reconstruction beyond the simple Fourier transform (for a few examples see [13–15]). An extension and further development of these ideas now pushes high-quality MRI acquisitions into the real-time regime. The approach presented here emerges as a combination of physical [16] and mathematical concepts [17] and provides serial images (i.e., MRI movies) at high signal-to-noise ratio (SNR), adequate spatial resolution and so-far unsurpassed temporal resolution [18,19].

## Methodologic considerations

Real-time imaging refers to the rapid and continuous acquisition of image data sets followed by image reconstruction and visualization – preferably without noticeable delay. This section addresses the choice of a physical method for real-time MRI acquisitions and then deals with a suitable reconstruction algorithm. In general, maximum speed is only achievable by reducing the amount of data that need to be acquired for any single frame of an image series

Future Medicine part of fsg

or MRI movie – a scenario typically described as 'undersampling'.

## ■ Real-time MRI acquisitions

There are three basic types of single-quantum proton NMR signals that may be employed for MRI: free induction decay signals in the form of a gradient echo, spin echoes and stimulated echoes, which may be excited by one, two or three successive RF pulses, respectively. Additionally, rapid pulse repetitions may lead to a complex overlap of coherence pathways that are referred to as steady-state free precession (SSFP) signal. For MRI the SSFP signal has to be ensured by fully balanced (i.e., symmetric) applications of magnetic field gradients that cancel all net gradient moments, and therefore result in a zero phase per repetition interval (TR). In general, all signal types may be applied for real-time imaging, but with different advantages and disadvantages.

Single-shot spin-echo (rapid acquisition with refocused echoes) [20] and stimulated echo MRI sequences [21] were described more than 25 years ago. However, both techniques are severely hampered for real-time applications because they usually excite the entire available longitudinal magnetization, and therefore do not easily offer continuous imaging at sufficient speed. Moreover, rapid stimulated echo sequences suffer from limited SNR, while repetitive rapid spin-echo sequences are restricted because of their large number of RF pulses (with large flip angles) and correspondingly high RF power deposition with the risk of tissue heating.

In order to guarantee high frame rates for dynamic acquisitions with echo-planar or spiral imaging sequences, respective gradient-echo rather than spin-echo versions have to be excited with flip angles much lower than 90°. This requirement severely reduces the attainable SNR normally exploited for single-shot imaging such as in multislice functional MRI with repetition times (TR) of 2 or 3 s. Long gradient-echo trains are also prone to magnetic inhomogeneity and susceptibility problems, which are unavoidable in many parts of the human body. It is therefore advantageous to use short-echo time short-TR gradient-echo MRI sequences for real-time imaging that are neither affected by RF power problems – even at high magnetic fields – nor very sensitive to tissue susceptibility differences.

Figure 1 shows a generic FLASH gradient-echo MRI sequence with radial encoding as used here for real-time imaging. Pertinent applications benefit from the highest possible receiver bandwidth for data acquisition, which typically is approximately 1000–2000 Hz/pixel. This choice ensures the shortest possible acquisition windows and echo times of approximately 1–2 ms and correspondingly short repetition times of approximately 2–3 ms, so that flip angles for RF excitation range from 5 to 10°.

In the native form as (spoiled) radial FLASH – and even without RF-spoiled excitation pulses – transverse coherences are effectively destroyed by the variable frequency-encoding gradients (from TR to TR) required for radial trajectories. The sequence therefore offers spin-density or $T_1$ contrast depending on the flip angle. On the other hand, the sequence may also be applied in conjunction with refocusing read gradients (refocused FLASH) or fully balanced gradients, which further include the slice-selection gradient (balanced SSFP). In these latter cases, the resulting image contrast shifts to a $T_2/T_1$ weighting.

The use of a radial rather than rectilinear (Cartesian) coverage of the data space is a preferred encoding option for real-time MRI for at least two reasons. First of all, radial trajectories only rely on frequency-encoding gradients that always cover both low- and high-spatial frequencies. For image reconstruction the inherent averaging of low spatial frequencies therefore avoids motion artifacts as caused by the use of phase-encoding gradients. Even more importantly, the continuous recording of all spatial frequencies with every single spoke renders radial imaging much more tolerant to undersampling. As a consequence, the number of spokes may be reduced without noticeable effect on the reconstructed image, whereas the removal of a data line in a Cartesian data set either results in image blurring (for outer lines) or aliasing (inner lines).

As indicated in Figure 1, for any given number of spokes, an advantageous acquisition scheme covers the full range of 360° in complementary views. Moreover, for dynamic MRI, acquisitions of successive images benefit from the use of interleaved sets of spokes. The example in Figure 1 schematically sketches three different sets of spokes (solid, broken and dotted lines), while experimental realizations typically employ five consecutive images with complementary sets of spokes.

## ■ Image reconstruction by regularized nonlinear inversion

Images from fully sampled or even moderately (e.g., twofold) undersampled radial data may be reconstructed by 'gridding' [22]. The gridding algorithm comprises a density compensation, convolution and rectilinear interpolation of the

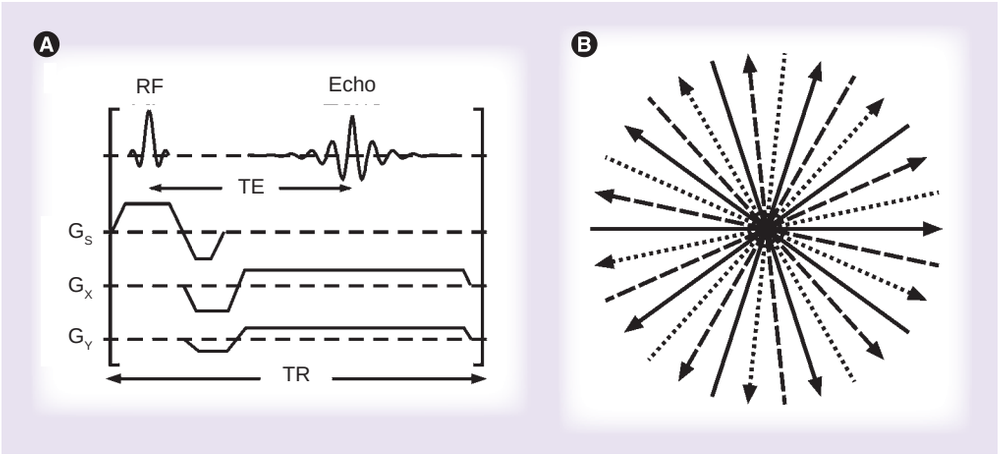


**Figure 1. Real-time MRI acquisition technique. (A)** Generic fast low-angle shot MRI sequence with radial encoding and **(B)** corresponding undersampled data space for three consecutive acquisitions with complementary sets of five spokes each (solid, broken and dotted lines). Echo: Gradient echo; $G_S$: Slice-selection gradient; $G_X$ and $G_Y$: Frequency-encoding gradients for radial encoding; RF: Radiofrequency; TE: Echo time; TR: Repetition time.

data with a Kaiser–Bessel kernel [23], an inverse fast Fourier transformation (FFT) and an image correction that accounts for the interpolation in data space. Unfortunately, this simple and fast algorithm fails for highly undersampled data sets, yielding images with severe streaking artifacts.

A solution to this problem stems from iterative algorithms that define the image as the solution of an inverse problem. Rather than using a direct inverse FFT of the data, iterative techniques estimate a starting image that then becomes optimized in several steps. This is accomplished by comparing the data of the actual image, which may be calculated by the forward solution of the problem (for MRI: a direct FFT), to the undersampled acquired data. A new improved image may then be estimated with the use of established methods in numerical mathematics. The principle is outlined in Figure 2. The specific method proposed here (see below) originally emerged as a nonlinear extension of conventional parallel imaging techniques [5,6] as it jointly estimates the desired image together with the sensitivity profiles of all RF coil elements used in a modern MRI acquisition [17].

In order to allow for a significant reduction of the necessary data, and thus achieve a corresponding speedup of the image acquisition process, a reconstruction technique for real-time MRI has to exploit the available information in an optimal way. An important building block is therefore parallel MRI, which at least partly restores the missing data with information about the spatially varying coil sensitivity profiles. Unfortunately, for higher acceleration factors than two to three, commercially available methods lead to artifacts that are mainly attributable to errors in the estimation of the coil sensitivities, which for a moving object change continuously. A second problem is the bad conditioning of the mathematical problem, which manifests itself in the amplification of noise for high degrees of undersampling.

A robust reconstruction technique for real-time MRI needs to address both issues. Problems caused by incorrect sensitivity profiles can be avoided in a mathematically precise formulation

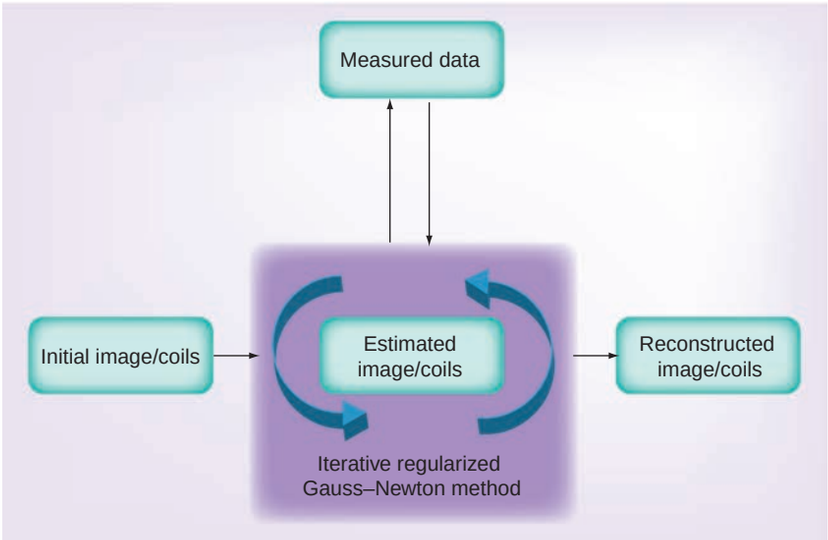


**Figure 2. The iterative algorithm for image reconstruction of highly undersampled MRI data sets.** The image and coil sensitivities for parallel MRI are defined as the solution of a nonlinear inverse problem, which is obtained by an iteratively regularized Gauss–Newton method. Starting from an initial guess, optimization of the estimated image is usually achieved within six to ten steps. In mathematical terms the badly conditioned problem may effectively be constrained by exploiting the temporal continuity of successive frames in a movie.

if autocalibrated parallel MRI is defined as a nonlinear inverse problem. While the solution of this problem requires the use of a computationally demanding iterative algorithm, this leads to an optimal estimation of image and coil sensitivities from all available data and has been shown to improve the image quality for high acceleration factors and small calibration areas [17]. While initially developed for conventional Cartesian sampling, the algorithm was extended to process data obtained with non-Cartesian sampling patterns and modified to be compatible with implementations on graphical processing units for more efficient computations [24].

To address the problem of increased noise, the range of possible solutions (i.e., image estimates that are in agreement with the acquired data) has to be constrained to sensible results by prior knowledge, which in mathematical terms refers to regularization. While variational penalties have successfully been used to regularize the reconstruction of static images from highly undersampled radial data [12,25], the redundancy inherent in a time series of images allows for a simpler and better solution: by penalizing the difference to the preceding frame with temporal regularization, missing high spatial frequencies can be restored from the preceding frame (acquired with a different spoke orientation). The strategy therefore effectively avoids a loss of spatial resolution for high degrees of radial undersampling. Although residual streaking artifacts may appear in fast moving areas of the image, where information from the previous frame is inconsistent with the current image, they may be removed by a median filter with a window size adapted to the periodicity of the sampling pattern. This emerges as a very efficient procedure because the remaining streakings are modulated by the periodic undersampling pattern, which results in a flickering appearance from frame to frame and differs from the actual image content. The streaking artifacts are easily identified as outliers and removed – a scheme which may be understood as a nonlinear version of the UNFOLD method [26].

Figure 3 presents an experimental validation of the described processing steps for the case of a systolic and diastolic frame from a short-axis heart movie. The series of reconstructions with gridding, basic nonlinear inversion as well as nonlinear inversion with additional temporal regularization and median filtering clearly demonstrates the achieved temporal fidelity. On the other hand, as with all methods that rely on prior knowledge, information that does not comply with the assumptions, will not correctly be recovered. However, the nonlinear nature of the median filter makes it possible to restore the original signal in many important situations (e.g., moving boundaries such as the myocardial wall or tissue interfaces) that cause a sudden jump

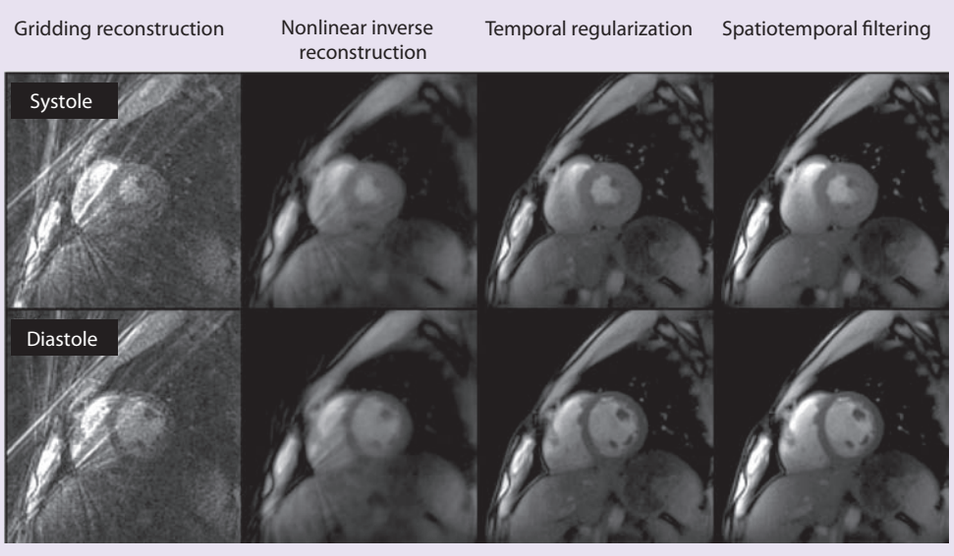


**Figure 3. Performance and temporal fidelity of the regularized nonlinear inverse reconstruction method.** (Top) Selected systolic and (bottom) diastolic frames of a real-time radial fast low-angle shot acquisition of the human heart (short-axis view) at 30 ms temporal resolution (15 spokes, repetition time/echo time = 2.00/1.29 ms, flip angle 8°, 2.0 × 2.0 × 8.0 $mm^3$). The reconstructions refer to conventional gridding as well as nonlinear inversion with additional temporal regularization and median filtering.

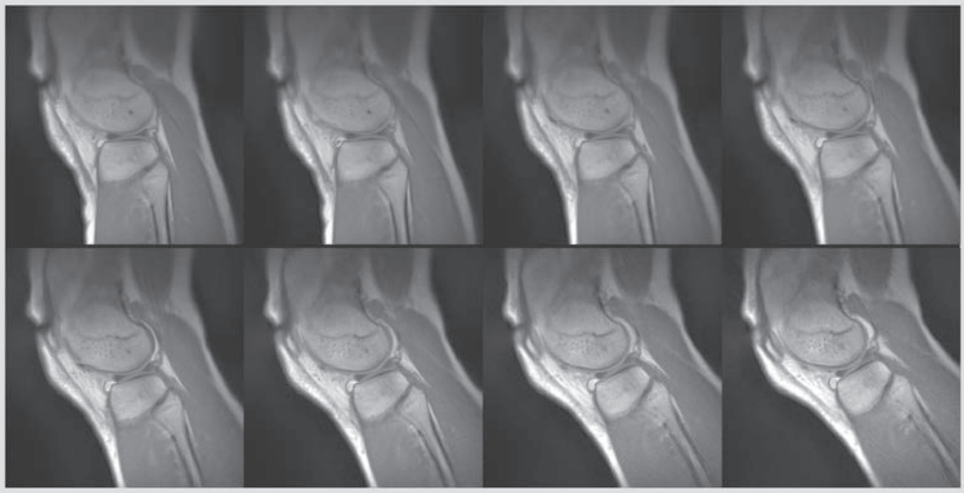

**Figure 4. Real-time MRI of voluntary knee bending after a mild contusion.** Selected frames taken every 4 s from (top and bottom) two different sections of respective movies at 333 ms temporal resolution (3 fps) acquired using refocused radial fast low-angle shot (73 spokes, repetition time/echo time = 4.56/2.30 s, flip angle 25°, 0.75 × 0.75 × 5.0 $mm^3$).

in the intensity of a pixel, where linear methods would often lead to temporal blurring.

## Applications

'The proof of the pudding is in the eating' – or in other words, the quality of a proposed method has to be demonstrated in real-world examples that are of scientific or medical relevance as well as offer new insights and opportunities for future applications. Real-time MRI of dynamic physiologic processes in humans therefore has to meet challenges such as adequate temporal resolution together with sufficient image quality (e.g., defined by SNR and spatial resolution), and further competes with alternative modalities such as x-ray techniques, ultrasound or endoscopy. This section deals with anatomic MRI studies in three different organ systems and respective imaging scenarios. All examples were obtained at and benefit from a magnetic field strength of 3T and further exploit the sensitivity of suitable multi-element RF coils.

### ■ Dynamic joint studies

A first area of application for real-time MRI refers to dynamic studies of moving joints. In most cases, pertinent movements may voluntarily be performed at only moderate speed, while the images often require a relatively high spatial resolution. Figure 4 shows a preliminary example of knee bending (two sections) of a subject suffering from a mild contusion. In this case, the delineation of fluid-filled spaces is emphasized by the choice of a refocused FLASH MRI sequence with $T_2/T_1$ contrast and an echo time that corresponds to in-phase conditions (positive overlap) for water and fat proton MRI signals. Laying in a prone position the subject slowly lifted the lower leg until reaching the inner bore of the magnet. The in-plane resolution was 0.75 mm, the slice thickness 5 mm and the temporal resolution 333 ms or 3 frames per second (fps). Signal reception was accomplished by wrapping a flexible 4-channel RF coil around the knee and fixing it with elastic bands. For clinical applications it will be possible to further reduce the number of spokes per frame to reach at least 200 ms acquisitions of 5 fps.

A related application at the same spatial resolution is the examination of the temporomandibular joint during voluntary opening and closing of the mouth. While an initial study still relied on a gridding technique with sliding-window reconstructions at lower temporal resolution [27], Figure 5 demonstrates selected views taken from a real-time MRI movie with true 200 ms image acquisition times or 5 fps (Supplementary Movie 1, see online www.futuremedicine.com/doi/suppl/10.2217/IIM.12.32). During the entire opening of the mouth, the relative positions of the mandibular condyle and articular disc are well depicted using refocused radial FLASH images and in-phase conditions. Such movies are expected to largely facilitate the diagnoses of temporomandibular joint disorders, which often involve internal structural derangements. They will replace pseudo-dynamic recordings with a bite block that controls the mouth-opening position in sequential step-by-step acquisitions. By contrast, dynamic imaging of an abnormal disc–condyle relationship and respective altered movements under

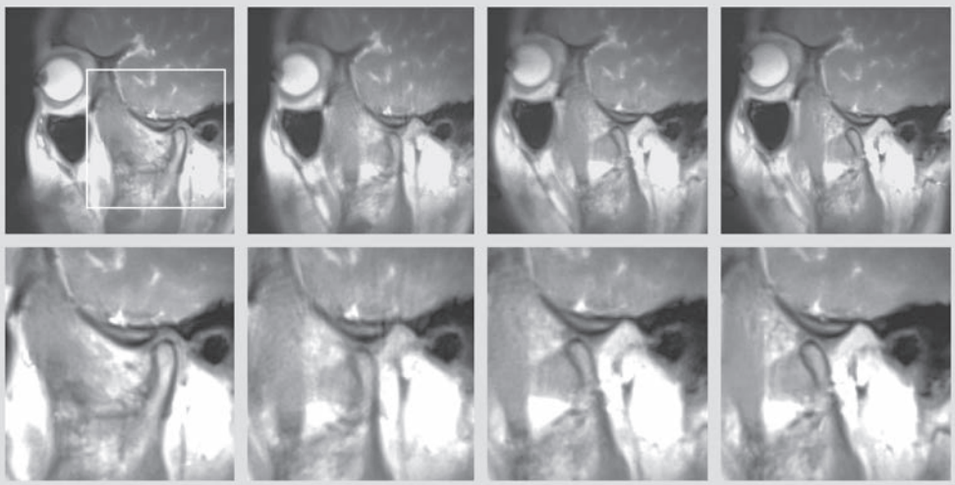

**Figure 5. Real-time MRI of the temporomandibular joint during voluntary opening of the mouth.** Selected frames (bottom: zoomed version) taken every 3.2 s from a respective movie at 200 ms temporal resolution (5 fps) acquired using refocused radial fast low-angle shot (45 spokes, repetition shot/echo time = 4.44/2.3 ms, flip angle 25°, 0.75 × 0.75 × 5.0 $mm^3$). See also **Supplementary Movie 1**.

voluntary muscular control will directly visualize the positions of the articular disc relative to the mandibular condyle and articular eminence. Such examinations are expected to identify the potential source of pain under realistic physiologic conditions.

## ■ Swallowing & speaking

Processes such as swallowing and speaking involve closely coordinated actions of multiple structures in the mouth and upper airways. Dynamic studies are challenging as movements of the lips, tongue, velum, epiglottis and larynx are very fast and are mostly performed without voluntary control. Real-time MRI of swallowing [28] and speaking [29], therefore, employs RF-spoiled radial FLASH MRI sequences with the shortest possible echo time (opposed-phase condition) and repetition time (~2.0–2.2 ms) as well as only 15–19 spokes. Typically, the best image quality is obtained by spin-density contrast with mild $T_1$ weighting (i.e., a low flip angle of 5°) and an in-plane resolution of 1.5 mm and slice thickness of 10 mm.

**Figure 6** shows selected frames from a movie of a single swallow of 5 ml pineapple juice, which serves as oral 'contrast' bolus because of its inherent concentration of paramagnetic manganese ions. Individual image acquisition times of 41.2 ms resulted in a temporal resolution of 24.3 fps. The different time points depicted in **Figure 6** refer to the oropharyngeal closure, velopharyngeal closure, glottal closure and esophageal opening, and further demonstrate the ascent of the larynx.

Although real-time MRI movies may be obtained in sagittal, coronal and axial orientation during multiple self-controlled swallows [28], the mid-sagittal plane turns out to be most valuable owing to its simultaneous coverage of the entire upper aerodigestive tract including the mouth, nasopharynx, pharynx, larynx and the uppermost gastrointestinal tract. These MRI movies provide detailed quantitative access to the timing, direction and efficiency (clearance) of swallowing as a prerequisite for clinical applications to dysphagia, which emerges as a serious sequelae in different neurologic diseases, as well as in functional disorders due to post-treatment deficits after surgery, radiotherapy or chemotherapy. Real-time MRI therefore bears the potential to compete with videofluoroscopy as the gold standard for swallowing diagnostics and may also be superior to flexible endoscopic evaluations, which, despite their reduced invasiveness, simplicity and low cost, suffer from a 'white out' during the important pharyngeal phase. Natural speech production, and in particular the dynamic visualization of the main articulators, is another important and in itself unique application for real-time MRI with straightforward extensions to singing or any other generation of sound (e.g., laughing, coughing, whistling or blowing an instrument). In a first study of German vowels, consonants and co-articulations during speaking of segments, words and sentences, even specific linguistic/phonetic questions such as the pre- and post-nasalization of vowels could be addressed by respective movements of the velum that control

the airflow through the mouth or nose [29]. Real-time MRI parameters are similar to studies of swallowing, but involve an even better temporal resolution of 33.3 ms or 30 fps (radial FLASH with 15 spokes). Supplementary Movie 2 shows a corresponding real-time MRI video with simultaneous audio recording of a subject speaking a long German sentence at natural speed after an initial fast swallow of saliva. The achieved image quality, spatiotemporal resolution and access to quantitative speaking parameters are expected to further advance applications in linguistics, clinical phonetics and logopedics.

## ■ Cardiac function

A most promising application for real-time MRI is cardiovascular imaging [19]. In comparison with established methods, which rely on ECG-synchronized acquisitions and merge data from multiple cardiac cycles, the advantages are manifold and comprise scientific, medical and even economic aspects. First of all, real-time MRI studies may be performed without breath holding, and therefore largely facilitate patient compliance, which in turn reduces the occurrence of failed examinations, improves image quality and enhances the diagnostic reliability. For similar reasons – complete motion robustness – the approach will be applicable to pediatric patient populations without the general need for anesthesia. Moreover, the ability to analyze multiple consecutive heartbeats for the first time offers access to the natural variances of functional parameters and their immediate responses to different physiologic conditions including exercise and stress. Real-time acquisitions are also a prerequisite for the examination of aperiodic phenomena, such as arrhythmia or turbulent blood flow, which are both chaotic in nature and therefore not amenable to synchronized data acquisitions from multiple cardiac cycles. Finally, a cardiac examination that can be based entirely on real-time MRI promises a much better cost–effectiveness, because it may be performed in a fraction of current examination times and without almost any patient-related failures.

Figure 7 and Supplementary Movie 3 depict an example of a short-axis movie of a healthy human subject at 34 ms temporal resolution or 30 fps (RF-spoiled radial FLASH using 15 spokes). While even higher frame rates are easily achieved at the expense of some spatial resolution, this version appears to be a good comprise for clinical trials as it offers 1.5-mm in-plane resolution and 6-mm section thickness. It should be noted that, apart from the achieved speed and image quality, the $T_1$ contrast of these recordings provides additional insights. The brightening of the MRI signal from the myocardial wall during systolic contraction (see Supplementary Movie 3) directly reflects the through-plane motion of the heart and may quantitatively be exploited in the future.

A corresponding 3-chamber view of the heart obtained with identical experimental parameters is shown in Figure 8 and Supplementary Movie 4. In this case, real-time MRI demonstrates access to new information about turbulent blood flow and the development of vortices within the heart chambers (here the left ventricle). Respective intensity patterns manifest themselves in magnitude images and are due to the inflow of blood from neighboring volumes. It remains to be seen whether flow-induced signal intensity changes can be related to computational fluid dynamics in order to learn more about the characteristics of turbulent flow *in vivo*.

Radial FLASH MRI of the heart as shown here at 3T is applicable at even higher magnetic fields. On the other hand, clinical studies mainly rely on SSFP contrast at a field strength of 1.5T. In fact,

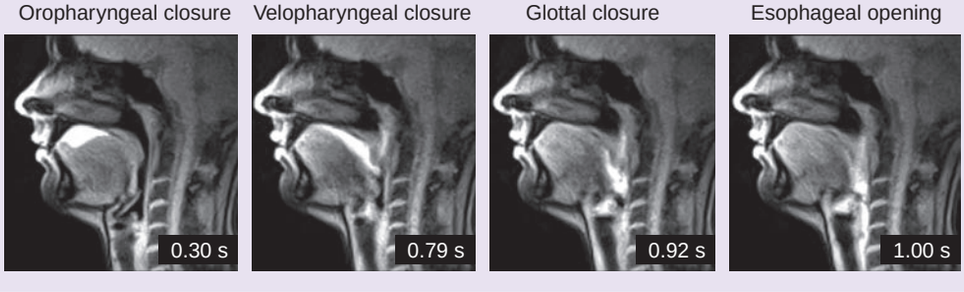


**Figure 6. Real-time MRI of natural swallowing using 5 ml pineapple juice as MRI 'contrast' agent.** Selected frames from a respective movie at 41 ms temporal resolution (24 fps) acquired using radial fast low-angle shot (19 spokes, repetition time/echo time = 2.17/1.44 ms, flip angle 5°, 1.5 × 1.5 × 10.0 $mm^3$). The images represent distinct swallowing events with relative timings to the beginning of the esophageal opening (i.e., 1.00 s). For a corresponding dynamic visualization of movements during speaking see Supplementary Movie 2.

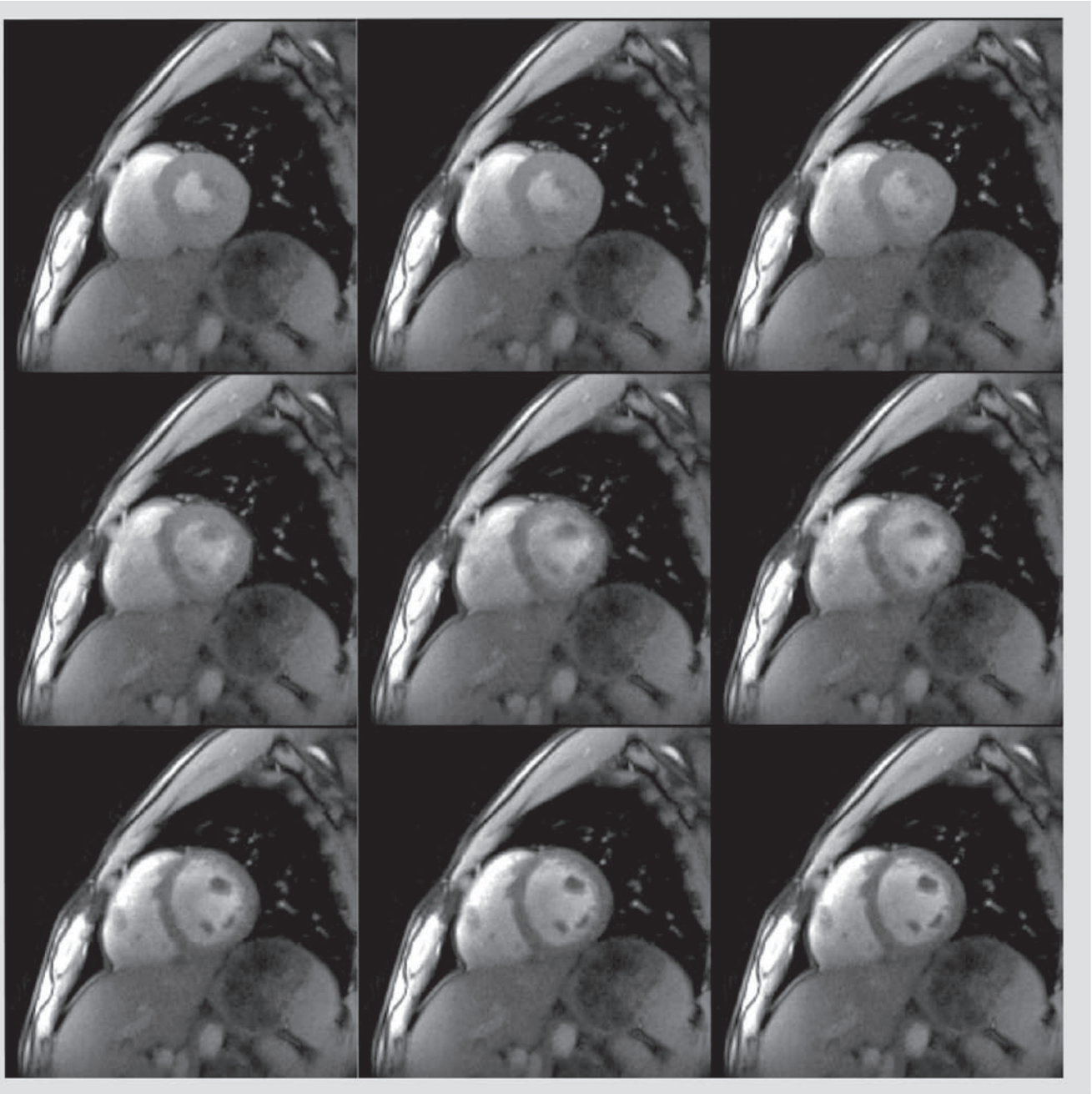

**Figure 7. Real-time MRI of the human heart in a short-axis view.** Consecutive frames (top left to bottom right) from a respective movie at 34 ms temporal resolution (30 fps) acquired using radial fast low-angle shot (15 spokes, repetition time/echo time = 2.28/1.46 ms, flip angle 8°, 1.5 × 1.5 × 6.0 $mm^3$). The images represent a 373-ms period of a single cardiac cycle from peak systole (top left) to early diastole (bottom right) demonstrating the rapid post-systolic expansion of the contracted and thickened myocardium. See also **Supplementary Movie 3.**

the proposed real-time MRI method also works with fully balanced radial gradients at this lower field (data not shown). Further optimized implementations will evaluate the accessible spatial and temporal resolution.

## Extensions

One of the reasons for the flexibility and versatility of MRI is the ability to exploit the basic MRI signal for encoding additional information. State-of-the-art MRI systems therefore present as a large toolbox with many diverse technical extensions and medical applications. Similar arguments hold true for MRI studies in real time. This section covers preliminary examples of extended real-time imaging methods that offer new information beyond mere anatomic insights.

## ■ Cardiovascular blood flow

A straightforward adaptation to real-time MRI is the use of flow-encoded phase-contrast principles for quantitative determinations of flow velocities in blood vessels. In its most simple and clinically most often applied version, the approach requires only two acquisitions with and without a bipolar velocity-encoding gradient in slice direction to assess the velocity of through-plane flow perpendicular to the imaging section. When these acquisitions are performed with undersampled radial FLASH and only a very low number of spokes, they allow for cardiovascular flow measurements in real time [30].

Figure 9 and Supplementary Movie 5 show the blood flow in the ascending aorta of a healthy subject as determined by a phase-contrast MRI sequence at 37 ms temporal resolution or 27 fps. The underlying images rely on two interleaved acquisitions each with only seven spokes (TR = 2.6 ms) and a bipolar gradient spanning a velocity field-of-view of ± 150 cm $s^{-1}$. The left-hand side of Figure 9 depicts a magnitude and corresponding phase-contrast image at systolic peak flow. The latter presents with bright intensities (i.e., high phase differences = high flow values) in the ascending aorta and shows a dark appearance of the descending aorta with blood flow in the perpendicular direction. Color-coded velocity profiles from a region-of-interest encompassing the ascending aorta are depicted in the right-hand side of Figure 9. They represent six consecutive frames (185-ms period) of a single cardiac cycle that demonstrate the decrease of flow velocities after systole and the deformation of the initially symmetric profile due to the back flow required for feeding the

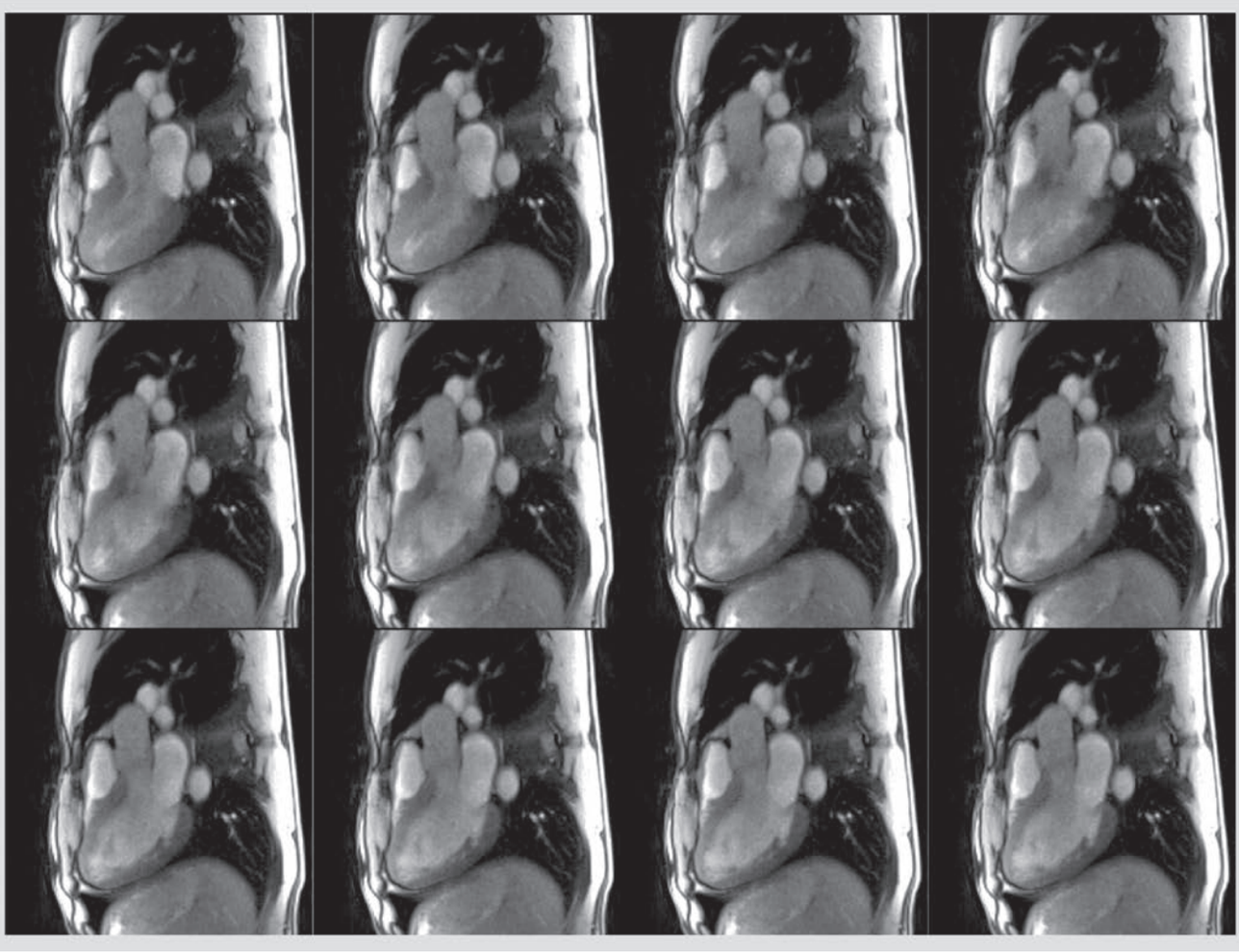

**Figure 8. Real-time MRI of the human heart in a three-chamber view.** Consecutive frames (top left to bottom right) from a respective movie at 34 ms temporal resolution (30 fps) acquired using radial fast low-angle shot (15 spokes, repetition time/echo time = 2.28/1.46 ms, flip angle 8°, 1.5 × 1.5 × 6.0 $mm^3$). The images represent a 373 ms period of a single cardiac cycle also demonstrating the development of turbulent blood flow in the left ventricle after opening of the mitral valve (top row). See also Supplementary Movie 4.

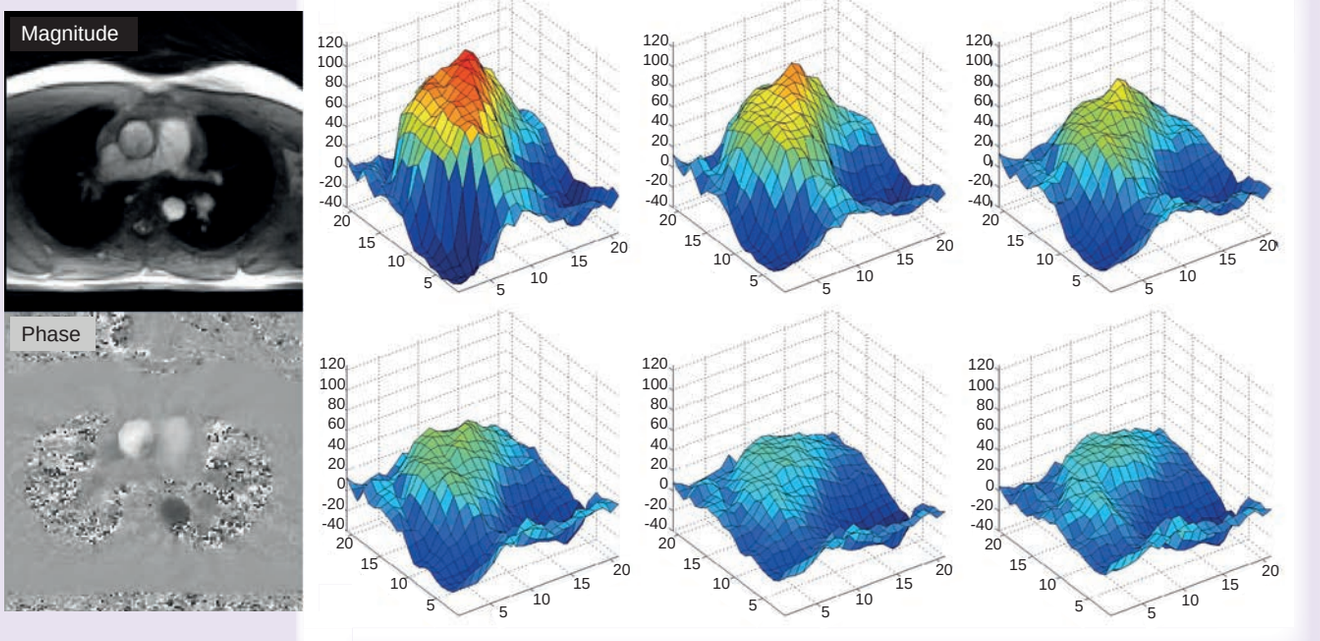


**Figure 9. Real-time MRI of blood flow velocities in the ascending aorta.** Magnitude and phase-contrast image (left) as well as six consecutive velocity profiles of the ascending aorta (right) taken from a respective phase-contrast MRI movie at 37 ms temporal resolution (27 fps) acquired using radial fast low-angle shot (2 × 7 spokes, repetition time/echo time = 2.64/1.84 ms, flip angle 10°, 1.8 × 1.8 × 6.0 $mm^3$) with and without a bipolar velocity-encoding gradient ($v_{enc}$ = 150 cm $s^{-1}$). The color-coded velocity profiles represent a 185-ms period of a single cardiac cycle demonstrating the rapid decrease of blood flow in the ascending aorta after systolic peak flow (here approximately 90–100 cm $s^{-1}$). The asymmetry of the profiles reflects the back flow (dark blue zone in right corner) feeding the coronary arteries. See also **Supplementary Movie 5**.

coronary arteries. **Supplementary Movie 5** visualizes the full dynamics of these velocity profiles for ten consecutive cardiac cycles.

It is expected that real-time access to flow parameters during free breathing offers new potential for the assessment of pathologic deviations or irregularities within single or serial heartbeats. Accordingly, clinical evaluations of real-time flow measurements in direct comparison to ECG-gated phase-contrast MRI and for all major heart vessels are currently in progress. On the other hand, it is also possible to extend the velocity-encoding to higher-order flow properties (e.g., acceleration or jerk) using suitable gradient waveforms or to combine velocity encodings along three orthogonal directions – although at the expense of a prolonged acquisition time. It remains to be seen whether future developments will achieve a temporal resolution below 50 ms for the determination of a 3D flow vector in a cross-sectional image. On the other hand, spatial coverage of the entire heart or aortic arch is unlikely to be performed in real time, but even such studies may benefit from the use of undersampled acquisition and reconstruction techniques.

## ■ Myocardial strain: tagging

Another simple extension of anatomic real-time MRI of the heart is the visualization of myocardial wall motion or strain by RF tagging (e.g., [31]. As demonstrated in **Figure 10** for a short-axis movie at 30 fps (same experimental conditions as for **Figures 7 & 8**) the method monitors the geometric distortion of a rectangular 2D saturation pattern in the myocardial wall due to systolic contraction and wall thickening. Spatially selective saturation is accomplished by RF excitation in combination with suitable gradients, which for the example in **Figure 10** saturates the magnetization at 8-mm distances within the two in-plane dimensions of the image. Presaturation modules only require a short amount of time and may be incorporated into the real-time MRI acquisition process without compromising the spatiotemporal resolution of the individual images. Following a single application the saturation pattern slowly fades away, because $T_1$ recovery leads to a re-equilibration of the steady-state MRI signal. In this preliminary study, tagging pulses were applied every 2 s during real-time MRI, while preferentially they are ECG-triggered at distinct cardiac phases.

## ■ Water–fat separation

The identification and separation of water and fat proton MRI signals is an important aspect with both technical and clinical implications. While multi-echo acquisition methods such as echo-planar and spiral imaging generally rely on frequency-selective excitation (or suppression) of either the water or fat component in order to avoid off-resonance image artifacts, clinical applications of water–fat separation benefit from the additional 'contrast' and more specific diagnostic insights.

In gradient-echo MRI, the destructive and constructive overlap of water and fat proton signals as a function of echo time is well known. It reflects the differential phase evolution of the field strength-dependent frequency difference and may be visualized in in-phase or opposed-phase images at specific echo times. For radial FLASH acquisitions in real time, in-phase conditions are chosen for joint studies as shown in Figures 4 & 5, while opposed-phase images are usually employed for cardiac studies with examples in Figures 7 & 8. In fact, the achievable speed may even be exploited for simultaneous acquisitions of both contrasts using dual-echo real-time MRI movies at 30 fps [19].

Apart from the use of preceding chemical shift-selective RF pulses [32], numerous algorithms have been developed to extract water-only and fat-only images from multi-echo recordings since the early work by Dixon [33]. In order to account for the unavoidable influence of magnetic field inhomogeneities (i.e., regional $T_2^*$ contributions), most current approaches use at least three gradient echoes – often with prescribed echo times. Figure 11 shows a respective real-time adaptation where a triple-echo radial FLASH sequence (45 spokes) is used to separate water and fat components for a study of knee movements. Water–fat separation was accomplished by analytical water–fat separation with safest first region growing [34]. For real-time imaging, the region growing is modified to take advantage of the phase from the previous frame, while the temporal median filter was only applied to the final separated image series.

## ■ Tissue characterization: $T_2^*$ mapping

The extension of the original two-point Dixon method to a triple-echo recording for water–fat separation lends itself to the development of a true multi-echo radial FLASH sequence for a full $T_2^*$ determination. A variety of body tissues are potential targets for the analysis of quantitative proton density and $T_2^*$ maps that may be obtained by fitting the multi-echo images to an exponential function. For example, internal structures of joints may be studied under different pressures during movement, while parameter maps for the myocardial wall may unravel differences during the cardiac cycle or in response to external physiologic conditions. A preliminary

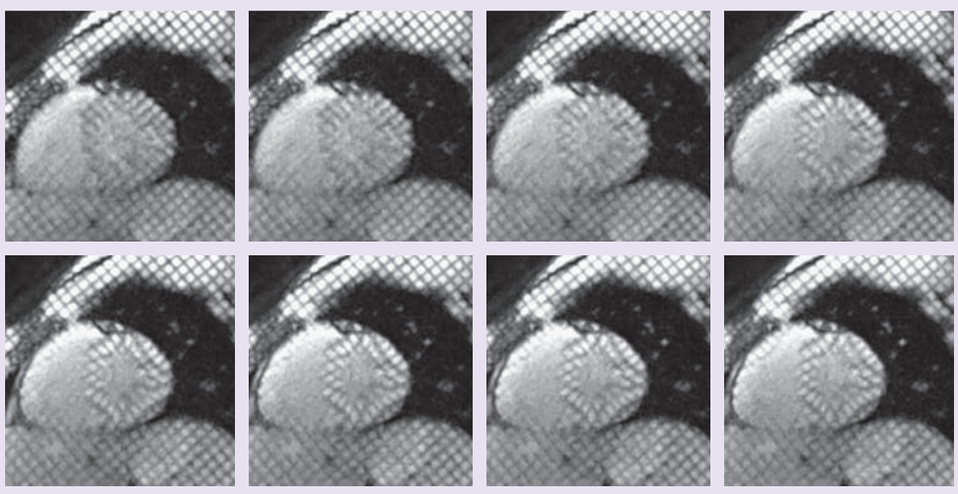

**Figure 10. Real-time MRI of the human heart (short-axis view) visualizing strain within the myocardial wall by tagging.** Consecutive frames (top left to bottom right) from a respective movie at 34 ms temporal resolution (30 fps) acquired using radial fast low-angle shot (15 spokes, repetition time/echo time = 2.28/1.46 ms, flip angle 8°, 1.5 × 1.5 × 6.0 $mm^3$) with additional tagging (2D spatial presaturation of the magnetization at 8 mm distances) every 2 s. The images represent a 239-ms period of a single cardiac cycle demonstrating the distortion of the applied rectangular saturation pattern in the myocardial wall (top left) due to subsequent systolic contraction and wall thickening (lower row).

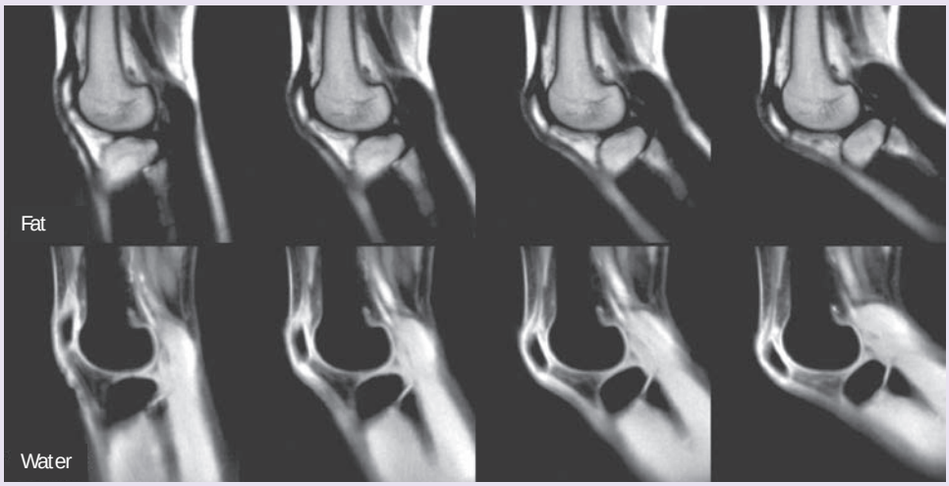


**Figure 11. Real-time MRI of knee movements with separation of (top) fat and (bottom) water components.** Selected frames obtained every 4 s from a respective movie at 250 ms temporal resolution (4 fps) acquired using triple-echo radial fast low-angle shot (45 spokes, repetition time/echo time = 5.50/1.78–3.16–4.54 ms, flip angle 12°, 1.0 × 1.0 × 5.0 mm$^3$). For further details see the 'Water–fat separation' section.

result for the human heart is shown in Figure 12, which depicts a proton density and $T_2$* map from peak systole and late diastole, respectively. The maps have been selected from respective proton density and $T_2$* movies obtained after fitting a single exponential to the individual images of a multi-echo real-time MRI acquisition. Because of the use of nine gradient echoes and despite a reduction of the image acquisition to only 9 spokes per frame, the acquisition time was 87 ms and must be considered too long for adequately resolving individual cardiac events. Nevertheless, dynamic access to motion-robust $T_2$* parameters at 11 fps may be beneficial for a variety of other organ systems.

Moreover, further progress is foreseeable as multi-echo radial FLASH sequences may employ different spatial encodings for different echo times, and thereby improve the temporal resolution by at least a factor of two. When pertinent data sets are subjected to a model-based reconstruction as previously developed for $T_2$ mapping from undersampled spin-echo MRI data [35,36], the two parameter maps may be directly calculated from the undersampled raw data. In other words, this mathematical approach exploits a known model function to determine related parameter maps without intermediate calculations of differently weighted images and subsequent fitting. It is much more efficient than conventional strategies and allows for accelerated, as well as quantitative, mapping. Future applications are likely to include $T_1$ mapping as well as extensions to perfusion and thermometry.

## ■ 3D localization: toward interventional MRI

Robust anatomic MRI studies in real time as well as dynamic assessments of tissue characteristics such as relaxation times, tissue perfusion or regional temperature pave the way to renewed interest in 'interventional' MRI. Another desirable feature in this context is the exact 3D localization of a surgical instrument used for a minimally invasive intervention. A surprisingly simple solution to this apparently unsolvable problem of '3D MRI in real time' stems from spatially encoded phase-contrast MRI [37]. In close analogy to flow-encoded phase-contrast MRI (compare Figure 9), the technique encodes a spatial position (rather than a velocity) along a perpendicular orientation of the imaging plane. It relies on a phase-difference map from two projection images obtained with and without a spatial phase-encoding gradient. The method therefore works best for 3D curved, but otherwise planar, objects such as a human hand or any other 2D or 1D object in space.

Figure 13 and Supplementary Movie 6 show an example of a water-filled tube in the form of a 3D spiral that is slowly retracted from its support. The experiment mimics the movement of a labeled 'catheter' inside a human body. The actual acquisition relies on two (interleaved) phase-sensitive projection images with and without a monopolar (rather than bipolar) phase-encoding gradient perpendicular to the projection plane. The phase information in the respective phase-contrast map (shown in the bottom planes of Figure 13) directly refers to the positions of the object along that

dimension. If the spatially encoded phase-contrast maps are obtained by real-time MRI, the resulting 3D representations of the object lead to 3D MRI movies at ms temporal resolution [37]. For future applications in interventional MRI pertinent localizations may advantageously be interleaved with anatomic imaging or parametric mapping. A distinction of the proton signals of a labeled instrument from those of the body may be achieved by exploiting differences in relaxation times or resonance frequency. On the other hand, it may be advantageous to combine spatial phase-contrast MRI with tracking of active guidewires by recording corresponding RF signals with a separate receive-only channel (e.g., [38]).

## Challenges

At this stage, the most important task for real-time MRI is a thorough clinical evaluation in various fields of application – a translational process that meets several important challenges. For example, while the use of real-time MRI in clinical practice is expected to immediately improve patient comfort and experimental robustness compared with traditional methods, its adaptation to and optimization for specific clinical questions requires the development of new study protocols and evaluations in direct comparison to established procedures. Moreover, in many cases real-time MRI acquisitions will not simply provide the same information in a more convenient way, but will instead require a different analysis and interpretation of the data. A typical example is real-time MRI of the heart where multiple heartbeats during free breathing lead to movies with hundreds of serial images, whereas current studies merge ECG-triggered data from multiple heartbeats, and therefore rely on the relatively simple analysis of a single cardiac cycle with approximately 20–30 images.

### ■ Volume coverage

Another important issue is the volumetric coverage of an entire organ. While real-time MRI inherently implies cross-sectional imaging, many applications benefit from or even require access to a larger 3D volume. To some extent, this is already possible with the present implementation, which allows for the simultaneous recording of movies from multiple sections in arbitrary geometric positions – in an interleaved or sequential acquisition mode and at the expense of temporal resolution, which restricts the approach to only a few sections. Even more sections may become available by the simultaneous excitation of multiple sections in conjunction with parallel MRI [39]. Alternatively, volumetric imaging may be achieved by the sequential recording of real-time movies that form a stack of sections encompassing, for example, the entire heart.

True real-time 3D MRI with sufficiently high spatial and temporal resolution remains an extremely challenging, if not impossible, task despite the fact that future 3D acquisitions may take advantage of parallel MRI along the third dimension, as well as of the enhanced redundancy in a 3D data set for further acceleration. Pertinent extensions of 2D radial acquisition schemes may either use a Cartesian phase-encoding gradient in the third dimension ('stack of stars' trajectory), or employ radial trajectories along all three dimensions. Because these variants differ with respect to implementation complexity, achievable spatio-temporal resolution and reconstruction time, all of these options are currently under investigation.

### ■ Dynamic image analysis

Clinical applications of real-time MRI will require the development or adaptation of suitable

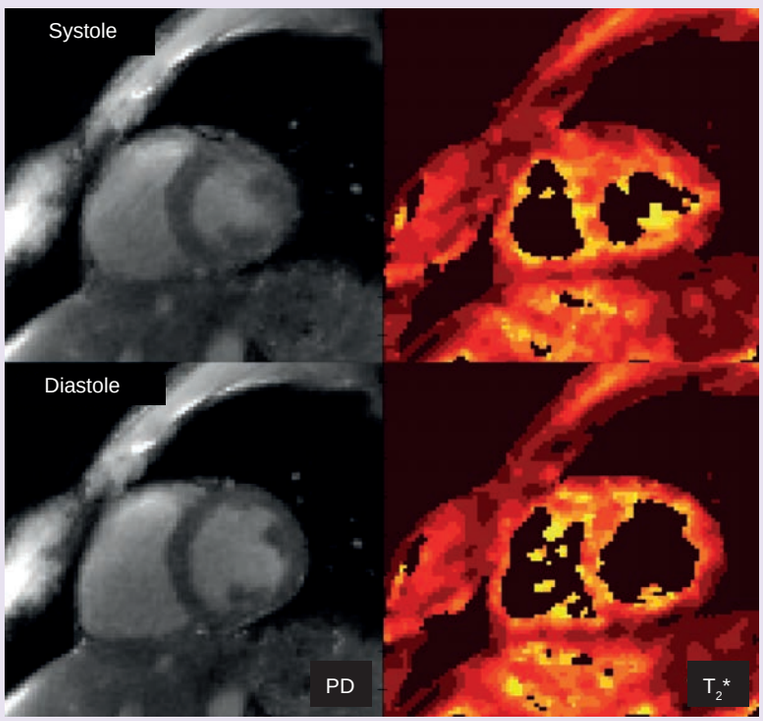


**Figure 12. Real-time proton density and $T_2$* mapping of the human heart (short-axis view).** Selected frames from (top) peak systole and (bottom) late diastole obtained from a respective multi-echo movie at 87 ms temporal resolution (9 × 11 fps) acquired using multi-echo radial fast low-angle shot (9 spokes, repetition time = 9.7 ms, 9 echoes, flip angle 15°, 2.0 × 2.0 × 8.0 mm$^3$). The color-coded $T_2$* maps cover relaxation times ranging from 10 ms (dark red) to 50 ms (yellow). For further details see the 'Tissue characterization: $T_2$* mapping' section.
PD: Proton density.

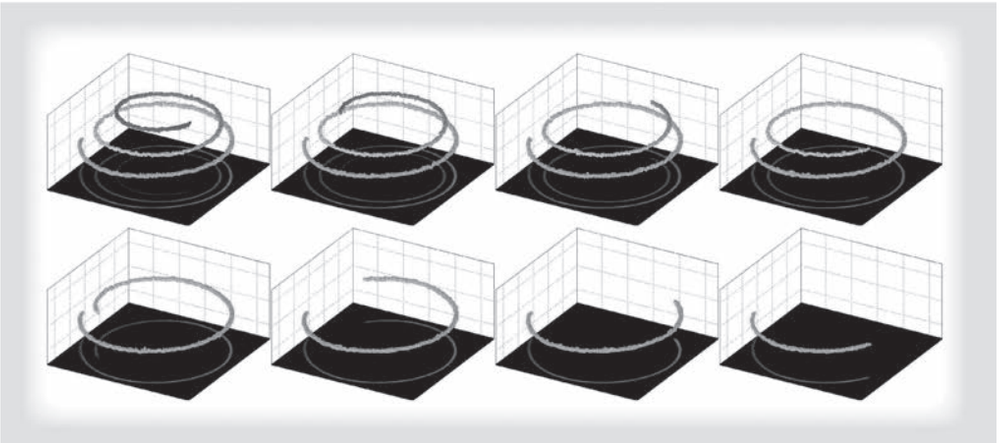

**Figure 13. Real-time 3D MRI of a water-filled tube by spatially encoded phase-contrast MRI.** Selected 3D views (top left to bottom right) of 2D maps taken every 2 s from a respective spatially encoded phase-contrast MRI movie at 44 ms temporal resolution (23 fps) acquired using radial fast low-angle shot (two × 11 spokes, repetition time/echo time = 2.00/1.28 ms, flip angle 12°, 1.5 × 1.5 mm$^2$). See also Supplementary Movie 6.

post-processing tools. This particularly applies to the analysis software commonly used for cardiovascular imaging. For example, existing methods for the evaluation of functional heart parameters only deal with images from a single cardiac cycle without respiratory influence. To fully realize the advantages of free breathing and access to physiologic variability, new software tools have to segment the myocardial wall in a time series of images from multiple cardiac cycles and further cope with the presence of breathing movements. The analysis of movies from different sections to generate a 3D model of the beating heart requires further coregistration techniques for a proper realignment despite breathing.

## ■ Mathematical developments

Although highly successful, the current mathematical framework for real-time MRI involves pragmatic choices that allow for computations in acceptable time as a prerequisite for preliminary trials on a commercial MRI system. For example, the temporal regularization only uses information from the previous frame, while more sophisticated schemes may estimate motion trajectories from a larger temporal window. Such approaches may lead to more accurate reconstructions and better spatial resolution, but are of course computationally more demanding, because they require a simultaneous estimation of all images in the reconstruction window.

Another pragmatic choice is the use of a temporal median filter as a post-processing step. Because the filter can be formulated as a L1 minimization problem, it should be possible to replace it by a suitable regularization term in the reconstruction itself. While it is not immediately clear whether this gives better results, such an implementation would also allow for an experimental optimization of other advanced regularization techniques. A related limitation of the current algorithm is the manual setting of the regularization parameter, although in practice the default parameters work reasonably well. Nevertheless, the performance might be improved by automatically finding the optimal regularization parameter (and corresponding stopping criterion) for each individual reconstruction. In principle, this idea might be extended to even locally adaptive parameters that depend on the properties of individual image regions.

## ■ Technical implementation

In principle, the implementation of the real-time MRI acquisition technique into an existing MRI system may be accomplished without changes to its hardware. However, the high computational demand of the reconstruction algorithm requires the use of special computation hardware equipped with several graphical processing units (GPUs) to achieve clinically feasible runtimes. While some MRI systems already use a single GPU for image reconstruction, the integration of multiple GPUs is currently not supported by any vendor. Initial clinical evaluations are expected to resort to a bypass computer, which receives the acquired data in real time over a computer network and feeds the reconstructed images back into the regular database of the host system for further processing and archiving. As shown before, such a system can be fully integrated into the scanner software. Our current prototype achieves frame rates of approximately 10 fps using four GPUs, and therefore allows for online reconstruction and immediate

display during scanning with acceptable delay. Foreseeable advances in computing hardware will not only remove the remaining limitations, but will also make it easier for vendors to provide the corresponding computation power as part of the MRI system.

## Conclusion

This work summarizes recent developments and first applications of a novel method for real-time MRI. The results are obtained on a human 3T MRI system and turn out to be superior to alternative trials in terms of image quality and temporal resolution as given by the true image acquisition time. The proposed techniques bear tremendous scientific and medical potential and are expected to alter the use of clinical MRI in a number of fields. A major area of application will be cardiovascular imaging of anatomy, function and blood flow.

## Future perspective

It is not unrealistic to assume that most of the aforementioned technical challenges will be met within the next 5 years. Pertinent developments will: add further robustness, image quality and diagnostic versatility; lead to widespread implementations on commercial MRI systems; and establish real-time MRI as a serious, if not mandatory, option for a widespread range of applications.

Apart from many diverse applications in monitoring joint dynamics or swallowing and speaking movements, future cardiovascular MRI studies are expected to be almost entirely based on real-time examinations during free breathing. Another area of relevance is interventional MRI, which may largely benefit from the techniques described here and further foreseeable developments.

More remote extensions of the principles underlying real-time MRI refer to studies that aim to improve efficiency. Examples include 3D MRI and the use of a moving patient table for volume coverage. Furthermore, the expected availability of sufficient computing power on commercial MRI systems will allow for dealing with more complex mathematical problems even outside the area of real-time MRI. An example will be the general adaptation of model-based reconstruction techniques to directly determine quantitative maps of model parameters from undersampled raw data sets in reduced measuring times.

### Acknowledgements

*The authors would like to thank their colleagues A Joseph, A Niebergall, S Schätz and M Untenberger, as well as their collaborators N Gersdorff, M Job, G Keydana, E Kunay, J Lotz and A Olthoff for valuable contributions and helpful discussions.*

### Financial & competing interests disclosure

*The authors have a financial interest in two pending patents related to the work described here. The authors have no other relevant affiliations or financial involvement with any organization or entity with a financial interest in or financial conflict with the subject matter or materials discussed in the manuscript apart from those disclosed.*

*No writing assistance was utilized in the production of this manuscript.*

### Executive summary

***Methodologic considerations***

- Undersampled radial gradient-echo sequences with image reconstruction by regularized nonlinear inversion provide a solution for real-time MRI.
- The approach offers good image quality and unsurpassed high temporal resolution for a variety of applications.

***Applications***

- Preliminary human studies promise considerable clinical opportunities.
- Cardiovascular MRI is expected to be entirely based on real-time MRI.
- Interventional MRI is expected to largely benefit from real-time MRI.

***Challenges***

- Remaining problems comprise variable contrasts, volume coverage, dynamic image analyses, mathematical improvements and technical implementations.
- Further progress of real-time MRI methods is foreseeable.

## References

Papers of special note have been highlighted as:
- of interest
- of considerable interest

1 Mansfield P. Real-time echo-planar imaging by NMR. *Br. Med. Bull.* 40, 187–190 (1984).

2 Ordidge RJ, Mansfield P, Doyle M, Coupland RE. Real time movie images by NMR. *Br. J. Radiol.* 55, 729–733 (1985).

3 Haase A, Frahm J, Matthaei D, Hänicke W, Merboldt KD. FLASH imaging. Rapid NMR imaging using low flip-angle pulses. *J. Magn. Reson.* 67, 258–266 (1986).

4 Frahm J, Haase A, Matthaei D. Rapid NMR imaging of dynamic processes using the FLASH technique. *Magn. Reson. Med.* 3, 321–327 (1986).

5 Sodickson DK, Manning WJ. Simultaneous acquisition of spatial harmonics (SMASH): Fast imaging with radiofrequency coil

arrays. *Magn. Reson. Med.* 38, 591–603 (1997).

6 Pruessmann KP, Weiger M, Scheidegger MB, Boesiger P. SENSE: sensitivity encoding for fast MRI. *Magn. Reson. Med.* 42, 952–962 (1999).

7 Ahn CB, Kim JH, Cho ZH. High-speed spiral-scan echo planar NMR imaging. *IEEE Trans. Med. Imaging* 5, 2–7 (1986).

8 Meyer CH, Hu BS, Nishimura DG, Macovski A. Fast spiral coronary artery imaging. *Magn. Reson. Med.* 28, 202–213 (1992).

9 Scheffler K, Hennig J. Reduced circular field-of-view imaging. *Magn. Reson. Med.* 40, 474–480 (1998).

10 Peters DC, Korosec FR, Grist TM *et al.* Undersampled projection reconstruction applied to MR angiography. *Magn. Reson. Med.* 43(1), 91–101 (2000).

11 Rasche V, de Boer RW, Holz D, Proksa R. Continuous radial data acquisition for dynamic MRI. *Magn. Reson. Med.* 34, 754–761 (1995).

12 Block KT, Uecker M, Frahm J. Undersampled radial MRI with multiple coils. Iterative image reconstruction using a total variation constraint. *Magn. Reson. Med.* 57(6), 1086–1098 (2007).

13 Lustig M, Donoho D, Pauly JM. Sparse MRI. The application of compressed sensing for rapid MR imaging. *Magn. Reson. Med.* 58(6), 1182–1195 (2007).

14 Lustig M, Donoho D, Santos JM, Pauly JM. Compressed sensing MRI. *IEEE Signal Proc.* 25, 72–82 (2008).

15 Mistretta CA, Wieben O, Velikina J *et al.* Highly constrained backprojection for time-resolved MRI. *Magn. Reson. Med.* 55, 30–40 (2006).

16 Zhang S, Block KT, Frahm J. Magnetic resonance imaging in real time – advances using radial FLASH. *J. Magn. Reson. Imaging* 31(1), 101–109 (2010).

▪ **Describes radial fast low-angle shot (FLASH) MRI as the basic acquisition technique for real-time MRI.**

17 Uecker M, Hohage T, Block KT, Frahm J. Image reconstruction by regularized nonlinear inversion – Joint estimation of coil sensitivities and image content. *Magn. Reson. Med.* 60(3), 674–682 (2008).

▪ **Describes regularized nonlinear inversion as a new reconstruction algorithm for parallel imaging.**

18 Uecker M, Zhang S, Voit D, Karaus A, Merboldt KD, Frahm J. Real-time MRI at a resolution of 20 ms. *NMR Biomed.* 23(8), 986–994 (2010).

▪▪ **Seminal work for real-time MRI. It describes for the first time all acquisition and reconstruction details as well as preliminary applications.**

19 Zhang S, Uecker M, Voit D, Merboldt KD, Frahm J. Real-time cardiovascular magnetic resonance at high temporal resolution: radial FLASH with nonlinear inverse reconstruction. *J. Cardiovasc. Magn. Reson.* 12, 39 (2010).

▪ **First application of the described real-time MRI method to cardiovascular imaging.**

20 Hennig J, Nauerth A, Friedburg H. RARE imaging. A fast imaging method for clinical MRI. *Magn. Reson. Med.* 3, 823–833 (1986).

21 Frahm J, Haase A, Matthaei D, Merboldt KD, Hänicke W. Rapid NMR imaging using stimulated echoes. *J. Magn. Reson.* 65, 130–135 (1985).

22 O'Sullivan JD. A fast sinc function gridding algorithm for Fourier inversion in computer tomography. *IEEE Trans. Med. Imaging* 4(4), 200–207 (1985).

23 Kaiser JF. Nonrecursive digital filter design using the $I_0$-SINH window function. *IEEE Int. Symp. Circuits Syst.* 20–23 (1974).

24 Uecker M, Zhang S, Frahm J. Nonlinear inverse reconstruction for real-time MRI of the human heart using undersampled radial FLASH. *Magn. Reson. Med.* 63, 1456–1462 (2010).

25 Knoll F, Clason C, Bredies K, Uecker M, Stollberger R. Parallel imaging with nonlinear reconstruction using variational penalties. *Magn. Reson. Med.* 67(1), 34–41 (2012).

26 Madore B, Glover GH, Pelc NJ. Unaliasing by Fourier-encoding the overlaps using the temporal dimension (UNFOLD), applied to cardiac imaging and fMRI. *Magn. Reson. Med.* 42(5), 813–828 (1999).

27 Zhang S, Gersdorff S, Frahm J. Real-time magnetic resonance imaging of temporomandibular joint dynamics. *Open Med. Imaging J.* 5, 1–9 (2011).

28 Zhang S, Olthoff A, Frahm J. Real-time magnetic resonance imaging of normal swallowing. *J. Magn. Reson. Imaging* 35(6), 1372–1379 (2012).

29 Niebergall A, Zhang S, Kunay E *et al.* Real-time MRI of speaking at a resolution of 33 ms: undersampled radial FLASH with nonlinear inverse reconstruction. *Magn. Reson. Med.* doi:10.1002/mrm.24276 (2012) (Epub ahead of print).

30 Joseph AA, Merboldt KD, Voit D *et al.* Real-time phase-contrast MRI of cardiovascular blood flow using undersampled radial FLASH and nonlinear inverse reconstruction. *NMR Biomed.* 25(7), 917-924 (2012).

▪ **First extension of the real-time MRI method to velocity-encoded phase-contrast MRI of cardiovascular blood flow.**

31 McVeigh ER, Atalar E. Cardiac tagging with breath-hold cine MRI. *Magn. Reson. Med.* 28, 318–327 (1992).

32 Haase A, Frahm J, Hänicke W, Matthaei D. $^1$H NMR chemical shift selective (CHESS) imaging. *Phys. Med. Biol.* 30, 341–344 (1985).

33 Dixon WT. Simple proton spectroscopic imaging. *Radiology* 153, 189–194 (1984).

34 Berglund J, Johansson L, Ahlström H, Kullberg J. Three-point Dixon method enables whole-body water and fat imaging of obese subjects. *Magn. Reson. Med.* 63, 1659–1668 (2010).

35 Block KT, Uecker M, Frahm J. Model-based iterative reconstruction for radial fast spin-echo MRI. *IEEE Trans. Med. Imaging* 28, 1759–1769 (2009).

▪ **Describes a model-based reconstruction technique for $T_2$ mapping.**

36 Sumpf TJ, Uecker M, Boretius S, Frahm J. Model-based nonlinear inverse reconstruction for $T_2$ mapping using highly undersampled spin-echo MRI. *J. Magn. Reson. Imaging* 34, 420–428 (2011).

37 Merboldt KD, Uecker M, Voit D, Frahm J. Spatially encoded phase-contrast MRI-3D MRI movies of 1D and 2D structures at millisecond resolution. *Magn. Reson. Med.* 66, 950–956 (2011).

▪ **First description of spatially encoded phase-contrast MRI and its application for 3D localization in real time.**

38 Kocaturk O, Kim AH, Saikus CE *et al.* Active two-channel 0.035" guidewire for interventional cardiovascular MRI. *J. Magn. Reson. Imaging* 30, 461–465 (2009).

39 Larkman DJ, Hajnal JV, Herlihy AH, Coutts GA, Young IR, Ehnholm G. Use of multicoil arrays for separation of signal from multiple slices simultaneously excited. *J. Magn. Reson. Imaging* 13(2), 313–317 (2001).